Human Molecular Genetics, 2017, Vol. 26, No. 6 1031–1040

doi: 10.1093/hmg/ddw391
Advance Access Publication Date: 20 December 2016
Original Article

ORIGINAL ARTICLE

Novel *UCHL1* mutations reveal new insights into ubiquitin processing

Siri L. Rydning[1,2,†,*], Paul H. Backe[3,4,†], Mirta M. L. Sousa[5], Zafar Iqbal[1], Ane-Marte Øye[6], Ying Sheng[6], Mingyi Yang[3,4], Xiaolin Lin[3,4], Geir Slupphaug[5,7], Tonje H. Nordenmark[8], Magnus D. Vigeland[6], Magnar Bjørås[2,3,5], Chantal M. Tallaksen[1,2,‡] and Kaja K. Selmer[6,‡]

[1]Department of Neurology, Oslo University Hospital, Norway, [2]Institute of Clinical Medicine, Faculty of Medicine, University of Oslo, Norway, [3]Department of Microbiology, Oslo University Hospital, Norway, [4]Department of Medical Biochemistry, University of Oslo, Norway, [5]Department of Cancer Research and Molecular Medicine, Norwegian University of Science and Technology (NTNU), Trondheim, Norway, [6]Department of Medical Genetics, Oslo University Hospital and University of Oslo, Norway, [7]Proteomics and Metabolomics Core Facility (PROMEC), NTNU, Trondheim, Norway and [8]Department of Physical Medicine and Rehabilitation, Oslo University Hospital, Norway

*To whom correspondence should be addressed at: Siri Lynne Rydning, Department of Neurology, Oslo University Hospital, Ullevål Hospital, PO Box 4956 Nydalen, N-0424 Oslo, Norway. Tel.: +47 23026443; Fax: +47 22118801; Email: s.l.rydning@medisin.uio.no

Abstract

Recessive loss of function of the neuronal ubiquitin hydrolase UCHL1 has been implicated in early-onset progressive neurodegeneration (MIM no. 615491), so far only in one family. In this study a second family is characterized, and the functional consequences of the identified mutations in *UCHL1* are explored. Three siblings developed childhood-onset optic atrophy, followed by spasticity and ataxia. Whole exome sequencing identified compound heterozygous variants in *UCHL1*, c.533G > A (p.Arg178Gln) and c.647C > A (p.Ala216Asp), cosegregating with the phenotype. Enzymatic activity of purified recombinant proteins analysed by ubiquitin hydrolase assays showed a 4-fold increased hydrolytic activity of the recombinant UCHL1 mutant Arg178Gln compared to wild type, whereas the Ala216Asp protein was insoluble. Structural 3D analysis of UCHL1 by computer modelling suggests that Arg178 is a rate-controlling residue in catalysis which is partly abolished in the Arg178Gln mutant and, consequently, the Arg178Gln mutant increases the enzymatic turnover. UCHL1 protein levels in fibroblasts measured by targeted mass spectrometry showed a total amount of UCHL1 in control fibroblasts about 4-fold higher than in the patients. Hence, studies of the identified missense variants reveal surprisingly different functional consequences as the insoluble Ala216Asp variant leads to loss of function, whereas the Arg178Gln leads to increased enzyme activity. The reported patients have remarkably preserved cognition, and we propose that the increased enzyme activity of the Arg178Gln variant offers a protective effect on cognitive function. This study establishes the importance of UCHL1 in neurodegeneration, provides new mechanistic insight about ubiquitin processing, and underlines the complexity of the different roles of UCHL1.

[†]The authors wish it to be known that, in their opinion, the first two authors should be regarded as joint First Authors.
[‡]The authors wish it to be known that, in their opinion, the last two authors should be regarded as joint Last Authors.
Received: September 12, 2016. **Revised:** November 8, 2016. **Accepted:** November 8, 2016

Introduction

Neurodegenerative disorders comprise a growing number of patients with progressive symptoms of neurological decline. Hereditary spinocerebellar disorders are a subgroup showing monogenic inheritance, and are characterized by progressive gait difficulties due to cerebellar ataxia and/or spasticity, sometimes with additional symptoms from the nervous system and/or other organ systems. Even in the era of high-throughput sequencing many cases remain unsolved (1,2).

Ubiquitin carboxyl-terminal esterase L1 (UCHL1) is one of the most abundant proteins in the brain, constituting 1–2% of the total soluble protein (3), and is highly expressed in neurons (4,5). The protein has hydrolase activities in the ubiquitin-proteasome pathway, and *in vitro* studies have also shown ubiquitin ligase activity (6). Variants in *UCHL1* have been implicated in the neurodegenerative disorders Parkinson's disease and Alzheimer's disease (7–10). UCHL1 is found to interact with amyloid β precursor protein (APP), and overexpression of UCHL1 might delay progression of Alzheimer's disease (7,11). The exact role of variants in *UCHL1* in Parkinson's disease has not been established. A rare heterozygous variant, Ile93Met, was reported in two siblings with autosomal dominant Parkinson's disease (12), but has still not been replicated 18 years later. Some evidence exists for an association between a relatively common polymorphism in *UCHL1*, Ser18Tyr, and Parkinson's disease, where both a decreased and an increased susceptibility have been suggested (8,9,13).

In 2013, the first family with a complex form of neurodegenerative disorder and a homozygous *UCHL1* variant was reported by Bilguvar *et al.* (MIM no. 615491) (14). They described three siblings of Turkish origin with childhood-onset neurodegeneration with optic atrophy, ataxia and spastic paraplegia. All had the homozygous Glu7Ala variant causing a loss of function of UCHL1. A similar phenotype is seen in *Uchl1* knockout mice (15). The present study reports the second family with *UCHL1* mutations showing a similar form of neurodegenerative disorder, thereby corroborating that UCHL1 dysfunction cause neurodegeneration. Moreover, the structural and biochemical consequences of the identified variants are explored, revealing new insight into the pathomechanisms of this disease and the many roles of UCHL1.

Results

Clinical description

The family was of Norwegian origin and the parents unrelated. The clinical features in the family were published as early as 1972, describing a monozygotic twin pair with the combination of spastic paraparesis and optic atrophy (16). Since then, the symptoms have been progressive, and a sister (III-4) has developed a similar phenotype (Fig. 1A). The clinical findings and results of supplementary investigations are reported in detail in Table 1, together with the results of examinations of the patients reported by Bilguvar *et al.* (14).

The monozygotic twins (III-5 and III-6) both developed neurological symptoms with progressive visual loss from 10 years of age and stiffness in the legs from 15 years of age. They became wheelchair-dependent from 55 years of age. The main findings at examination at age 62 were pronounced spasticity with contractures of all joints in the lower limbs, bilateral optic atrophy, tetraparesis, most pronounced in the lower limbs, inverted plantar responses, generalized fasciculations, intention tremor in hands, bilateral gaze-evoked horizontal nystagmus, severely reduced superficial and dorsal column sensibility, and high scores in Spastic Paraplegia Rating Scale (SPRS) (17) and Scale for Assessment and Rating of Ataxia (SARA) (18) (Table 1). Neuropsychological testing in the 1970s showed verbal IQ of 125 (III-5) and 115 (III-6), and performance IQ of 75 (III-5) and 82 (III-6) in the Wechsler Adult Intelligence Scale (WAIS) (16). Neuropsychological evaluation of the twins was repeated at age 63 using relevant tests from WAIS IV, Wechsler Memory Scale, California Verbal Learning Test and Delis-Kaplan Executive Function System. They both had conspicuously well preserved working memory and memory functions, 0.5–2.67 standard deviations above norm. Executive functions and language functions were within the normal range.

Patient III-4 developed severe myopia from 10 years of age, and eye examination at age 55 showed pale optic discs consistent with bilateral optic atrophy. She also developed severe "no-tremor" of the neck and positional and kinetic tremor of the upper limbs from the age of 20. Cerebellar ataxia of gait and extremities was first noted at clinical examination at the age of 54. Main findings at examination at 65 years of age were cerebellar ataxia without spasticity, reduced sensation for all modalities, nystagmus, disrupted saccades and facial myokymias. EMG/neurography of the twins at age 62 showed sensorimotoric neuropathy of axonal type, mainly in the lower limbs, progression from earlier examination and chronic re-innervation as well as denervation suggestive of a still ongoing process. Magnetic resonance imaging (MRI) of the three siblings showed atrophic optical nerves, without significant cerebellar atrophy, although patient III-5 had mild atrophy of the superior vermis (Fig. 1B and C).

There was no other history of visual loss, cerebellar ataxia or spasticity in the family, but the mother (II-2) and one sibling (III-1) had a tremor. The mother reportedly had a severe tremor of her head, neck and upper limbs starting after 50 years of age. The sibling (III-1) had a progressive tremor in the neck and upper limbs from young adult age, but no signs of upper motor unit involvement or cerebellar involvement at examination at age 74. The sister III-2 had previously been successfully treated for both ovarian cancer and malignant melanoma, neurological examination was unremarkable at age 74.

Whole exome sequencing identified UCHL1 *variants*

By whole exome sequencing, we identified two missense variants in *UCHL1* carried by both the affected III-4 and III-6: NM_004181.4(UCHL1):c.533G > A (p.Arg178Gln) and c.647C > A (p.Ala216Asp). There were no other likely pathogenic variants compatible with recessive inheritance, after filtering the exome data down to nonsynonymous or loss-of-function PASS variants with allele frequencies less than 1% in the public databases 1000 Genomes, ESP5400 and ExAC. The sister III-4 was also analysed for variants in 177 candidate genes associated with autosomal dominant tremor, without identification of any variants considered to be likely pathogenic. Sanger sequencing confirmed that individuals III-4, III-5 and III-6 all were heterozygous for both missense variants. Family members III-1 and III-3 were homozygous for the wild type (WT) alleles, and the sibling III-2 was heterozygous for the c.533G > A (p.Arg178Gln) variant, supporting that the two variants are *in trans*. The two missense variants were not found in the databases ESP, dbSNP, 1000 Genomes, ClinVar or HGMD, nor in the 961 controls. In ExAC, a database of about 60.000 exomes, the c.647C > A (p.Ala216Asp) variant was absent, while the c.533G > A (p.Arg178Gln) variant was reported heterozygously in 10 individuals, representing a

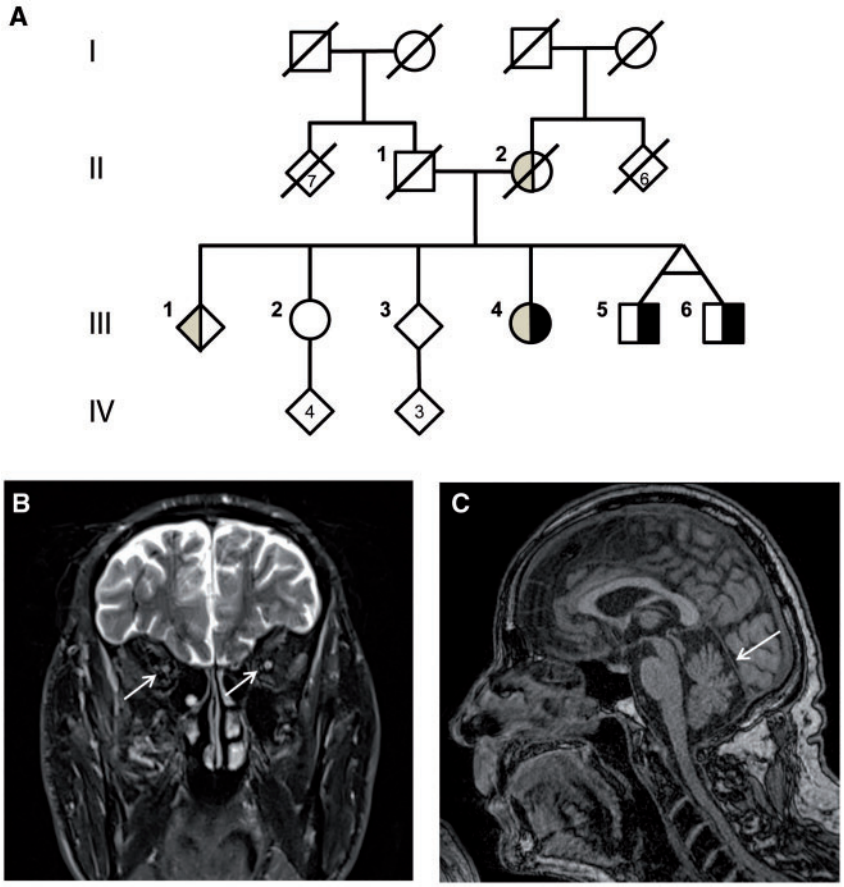

Figure 1. Pedigree and brain MRI. (**A**) Pedigree of the family. Black symbol = affected with spastic ataxia and optic atrophy; grey symbol = affected with tremor; square = male; circle = female; diamond = masked gender (for anonymization purposes); diagonal line = deceased. (**B** and **C**) Brain MRI of patient III-5 at age 63: (**B**) Coronal T2 image showing optical atrophy (arrows), and (**C**) midsagittal T1 image showing mild atrophy of the superior vermis (arrow).

very low frequency. There were no homozygous or compound heterozygous variants in *UCHL1* in 113 probands with pure or complex hereditary spinocerebellar disorders.

UCHL1 Arg178Gln results in increased hydrolytic activity

We analysed the effects of the Arg178Gln mutation on C-terminal hydrolase enzymatic activity by expressing and purifying the recombinant WT UCHL1 and Arg178Gln mutant in *E. coli*. The enzymatic activity of the mutant was then compared with that of the WT in an assay with ubiquitin-AMC as substrate. The ubiquitin-AMC cleavage was continuously monitored. Notably, Fig. 2 shows that the activity of the Arg178Gln mutant is increased about 4-fold compared to WT UCHL1. Overexpression of the Ala216Asp UCHL1 mutant resulted in inclusion bodies containing presumably misfolded, aggregated protein, thus the activity assays of this mutant was not possible.

Structural analysis of the UCHL1 Arg178Gln and Ala216Asp mutant proteins

Structural analyses of the Arg178Gln and Ala216Asp mutants were based on the previously determined crystal structure of human UCHL1 at 2.4 Å resolution (PDB ID: 2ETL) (19). The UCHL1 overall structure is typical for the papain family of cysteine proteases, comprising two lobes of five and two helices, respectively. The active site lies between the lobes in a relatively deep cleft where we find the catalytic triad consisting of Cys90, His161 and Asp176.

The positively charged Arg178 is placed directly above the catalytic triad and is engaged in an intricate network of direct and water-mediated hydrogen bonds within the active site. Sequence alignments show a high conservation for the positively charged arginine in this position. A column of four tightly bound water molecules forms a wedge that penetrates into the core of the protein and splits His161 apart from Cys90, disrupting the classical catalytic His-Cys diad (Fig. 3A). As previously mentioned by Das *et al.*, (19) the hydrogen-bonding network involving water molecules and the residues Glu60, Asn159, His161, Asp176 and Arg178 is absent in UCHL1 homologs like UCHL3 and Yuh1, and these differences may explain the observed low *in vitro* activity of UCHL1 compared to its homologs.

Ala216 is placed in the 6-stranded β-sheet and is one of several hydrophobic amino acids constituting a hydrophobic core between the β-sheet and the α-helix α7 (Fig. 3B). In the Ala216Asp mutant, the negatively charged and hydrophilic side chain may destabilize the folding of the protein and cause aggregation.

Quantification of UCHL1 mutant proteins in patient fibroblasts

Mass spectrometry-based proteomics is the most powerful strategy for the identification, characterization and quantification of

Table 1. Clinical findings and results of supplementary investigations in the patients in this study (patients III-4, III-5 and III-6), and in the patients described by Bilguvar *et al.* (NG 1024-1, NG 1024-2, NG 1024-3) (14)

	Patient III-4	Patient III-5	Patient III-6	NG 1024-1[a]	NG 1024-2[a]	NG1024-3[a]
Age at examination	65	62	62	28	33	34
Age at onset	10	10	10	5	7	5
First symptom	Visual loss	Visual loss	Visual loss	Visual loss	Visual loss	Balance problems
Vision	0,1 o.u.	Light perception	Light perception	–	–	–
Optical atrophy	+	+	+	+	+	+
SPRS	13	44	45	na	na	na
SARA	18	27	26	na	na	na
Standing without assistance	–	–	–	–	–	–
Gaze evoked nystagmus	+	+	+	+	+	+
Head titubation	+	–	–	+	+	+
Postural tremor	+	–	–	na	na	na
Intention tremor UL	+	+	+	na	na	na
Brisk deep tendon reflexes (UL/LL)	–/+	–/+	–/+	+/+	+/+	+/+
Inverted plantar responses	–	+	+	+	+	+
Hoffman responses	–	–	–	+	–	–
Grade of reduced muscle strength (UL/LL)	Mild/mild	Mild/severe	Mild/moderate	Normal/mild	Normal/mild	Normal/mild
Impaired superficial sensation (UL/LL)	–/+	–/+	–/+	+/+	+/+	+/+
Impaired positional sense	+	+	+	+	+	+
Impaired vibration sense (UL/LL)	–/+	–/+	–/+	+	+	+
Spasticity LL	–	+	+	+	+	+
Abnormal cerebellar tests, dysmetria (UL/LL)	+/nt	+/nt	+/nt	+	+	+
Ophthalmoplegia	–	Paresis upward gaze	–	na	na	na
Hand myotonia	–	–	+	+	–	–
Myokymia	+	–	–	na	na	na
Cognitive impairment	–	–	–	na	IQ 74	IQ 71
Fasciculations	–	+	+	na	na	na
Pectus carinatum	–	+	+	na	na	na
Pes cavus	+	+	+	na	na	na
EMG/neurography (age[b])	Chronic neurogenic axonal changes (65)	Axonal sensorimotor neuropathy (62)	Axonal sensorimotor neuropathy (62)	Normal nerve conduction velocity, myokymic activity (in all)		
Brain MRI (age[b])	Optic atrophy (63)	Optic atrophy. Mild cbl.atr. (63)	Optic atrophy (62)	Bilateral optic nerve and chiasm atrophy, Wallerian degeneration of the optic radiations, cbl. and mild cerebral atr. (in all)		
Visual evoked potentials (VEP) flash	na	Inc. lat., red. amp.[c]	Inc. lat., red. amp.[c]	Nearly absent response o.u. (in all)		
VEP electroretinogram	na	Normal	Normal	Normal	Normal	Normal
Muscle biopsy (age[b])	Normal (56)	na	Chronic denervation (48)	na	na	na

[a]Examination findings in patients NG 1024-1, NG 1024-2 and NG 1024-3 are adapted from Bilguvar *et al.*, including Supporting Information.

[b]Age at examination, in years.

[c]Increased latency time and reduced amplitude both eyes. LL = lower limbs; UL = upper limbs; – = absent; + = present; o.u. = both eyes; cbl.atr. = cerebellar atrophy; nt = not testable; na = not available.

proteins and peptides. Here, we employed a targeted mass spectrometry approach named parallel reaction monitoring (PRM) to identify and quantify the level of UCHL1 protein in control and patient fibroblast cells. Due to its high selectivity and sensitivity, PRM enables the detection and quantification of specific peptides from preselected protein targets in complex samples (reviewed in (20–22)). The high resolution and accuracy of the technique allows the distinction between UCHL1 WT peptides and UCHL1 peptides carrying a single mutation.

The total level of UCHL1 in patient fibroblasts was about 25–35% of the level in control fibroblasts (Fig. 4A). UCHL1 peptides containing Arg178 were detectable only in control cells whereas Arg178Gln was present only in patient cells (Fig. 4A), demonstrating that the patient cells only express the mutant protein and no wild type. UCHL1 peptides containing Ala216 were detectable in both control and patient cells, but the patient's cells displayed 25% expression as compared to control cells, whereas Ala216Asp was detectable in neither control nor patient cells. Thus, the

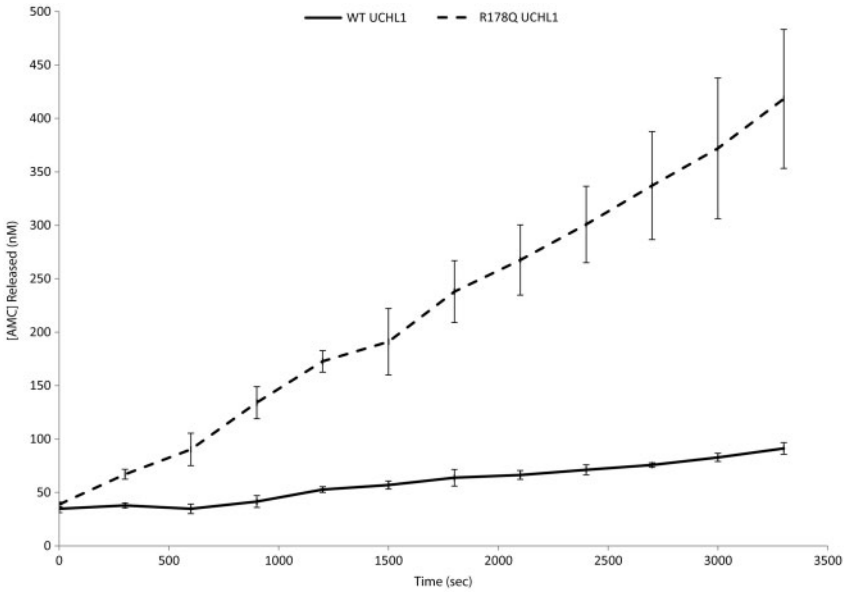

Figure 2. Enzymatic activity assay. Comparison of the enzymatic activity of WT UCHL1 and the Arg178Gln (R178Q) mutant protein ($n = 3$). Real time release of fluorescent AMC is shown for WT UCHL1 (black line) and Arg178Gln UCHL1 (dashed line). The substrate and enzyme concentrations for all reactions were 2500 and 4 nM, respectively.

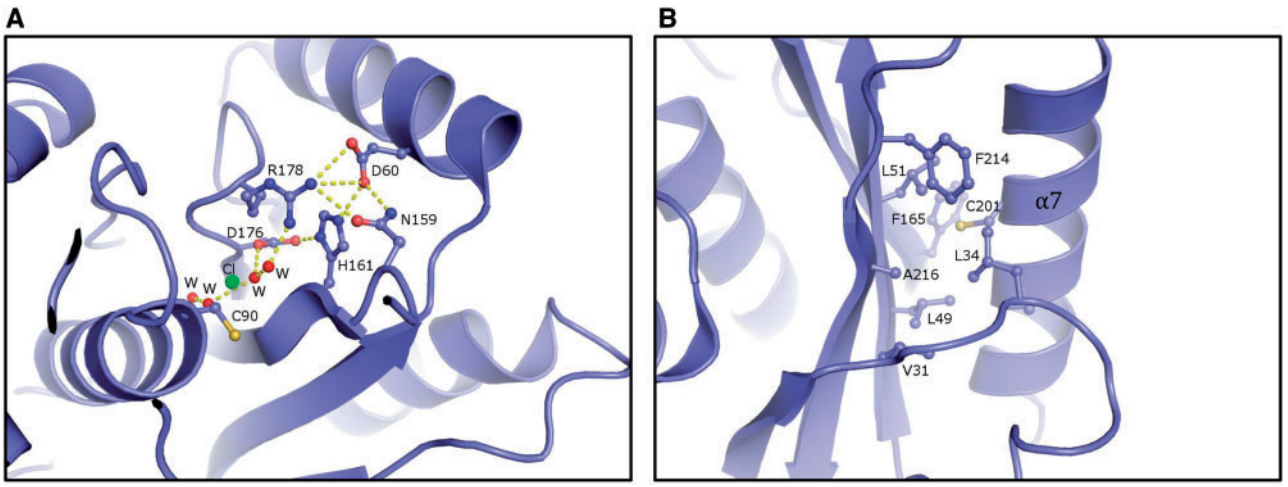

Figure 3. The crystal structure of human UCHL1 (19). (**A**) Close-up of the hydrogen pattern in the vicinity of Arg178 close to the catalytic triad. (**B**) Close-up of the hydrophobic core between the β-sheet and the α-helix α7. Ala216 is one of several hydrophobic amino acids constituting the hydrophobic core. The figure was made using the program PyMol [DeLano, W.L. The PyMOL Molecular Graphics System (2002) DeLano Scientific, San Carlos, CA, USA.].

patient's cells only express a stable protein of the UCHL1 Arg178Gln mutant and not the Ala216Asp mutant, indicating that the Ala216Asp mutant protein may be degraded or not expressed at all. Finally, sequencing of UCHL1 cDNA synthesized from patient mRNA indeed showed that Ala216Asp UCHL1 mRNA is present in the patient's cells (data not shown), supporting that the lack of the mutant protein is not due to degradation of UCHL1 transcripts in the patient's cells.

Discussion

This is the second report of a family with recessive early-onset progressive neurodegeneration with optic atrophy (MIM no. 615491) and mutations in *UCHL1*, confirming and elaborating the phenotype-genotype correlation. Three siblings (Fig. 1A) presented with childhood-onset visual loss as the first symptom, but their subsequent disease course differed, with either mainly pyramidal symptoms or late-onset cerebellar ataxia. The evaluation of the inheritance pattern in this family was complicated by the presence of tremor in the neck and upper limbs in two of the siblings and the mother (Fig. 1A). Sibling III-1 had WT alleles for the Arg178 and Ala216 UCHL1 positions, making it likely that the tremor was an additional, independent trait in this family, a good example of phenotype as a red herring. Similar to the patients described by Bilguvar *et al.*, the three affected siblings in this study exhibited symptoms mainly from both pyramidal and cerebellar pathways (Table 1). The Norwegian patients had more severe impairment of dorsal

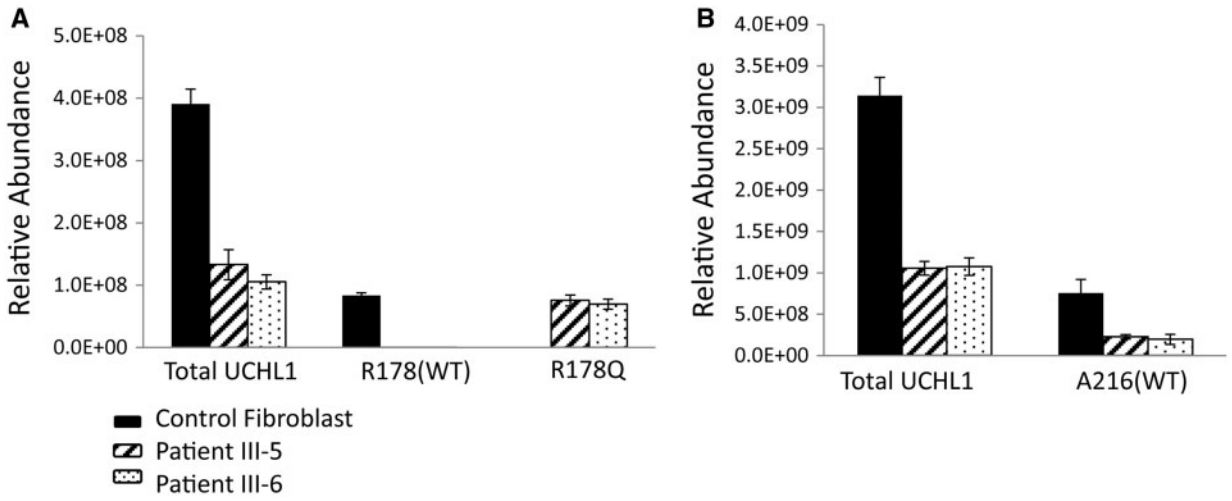

Figure 4. Quantification of wild type (WT) and mutated UCHL1 protein in fibroblast samples from patients. Relative abundance of total UCHL1 protein was calculated by summing the peak area values of 4 unique UCHL1 peptides for each sample. Levels of WT Arg178 and Ala216 and mutant Arg178Gln correspond to peak areas of single peptides carrying the respective residues. (**A**) Quantification of peptides containing the residue Arg178 (WT UCHL1) and the point mutation Arg178Gln was achieved through enzymatic digestion using Glu-C. (**B**) Quantification of the peptide containing the Ala216 (WT UCHL1) residue was performed via tryptic digestion. Peptides containing the mutation Ala216Asp were not detectable in trypsin- or Glu-C treated samples. Protein and peptide area values are normalized against β-actin levels. Error bars represent standard deviation from 3 technical replicates. Black = control fibroblasts; stripes = patient III-5; dots = patient III-6.

columns and peripheral nerves, possibly due to longer disease duration. Our findings further support the increasingly acknowledged importance of functional UCHL1 in both the central and the peripheral nervous system, as well as in the neuromuscular junction (15,23). Moreover, UCHL1 is also suggested to be implicated in Parkinson's disease, but the exact role is still debatable (6,9,13,24). The patients in this study and the previous study (14) did not exhibit typical parkinsonistic features.

Optic atrophy is a distinct finding in neurodegeneration, usually due to disrupted mitochondrial function, such as in SPG7, OPA1 and Leber hereditary optic neuropathy (25–28). SPG7 is one of the many neurodegenerative disorders with a broad clinical spectrum, with symptoms ranging from autosomal recessive spastic ataxia with progressive ophthalmoplegia to autosomal dominant pure cerebellar ataxia (29–31). Over the years extensive investigations were done to identify the molecular diagnosis in the family in this study, in particular SPG7 and mitochondrial disorders were regarded to be likely differential diagnoses. However, they were proven wrong, and we did not find signs of mitochondrial dysfunction. Thus, mitochondrial involvement in the pathogenesis of UCHL1-related neurodegeneration remains to be confirmed.

The ubiquitin-proteasome pathway plays an important role in the removal of damaged proteins in the cell, a process proven to be essential to maintain cell homeostasis and when dysfunctional, leading to severe disorders of the central and peripheral nervous system (23,32–34). The proposed role of UCHL1 is mainly to maintain the pool of monoubiquitin for use in ubiquitinylation reactions. To explore the underlying pathomechanisms of the identified variants, functional analyses were performed. Analyses revealed unexpectedly complex results as the Arg178Gln variant led to the increased hydrolytic activity and the Ala216Asp variant was non-soluble. Mass spectrometry showed a UCHL1 concentration of 25–35% in patient fibroblast cells compared with controls, and that only the Arg178Gln variant was expressed. Enzyme activity analyses showed that the Arg178Gln variant had a 4-fold increased hydrolytic activity. This increased catalytic turnover of the Arg178Gln mutant suggests that Arg178 is a catalytic rate-controlling residue in UCHL1 and that it plays a central role keeping the intricate hydrogen-bonding network of UCHL1 intact. This "parking brake" mechanism might be important to regulate the activity of the protein and thereby the enzyme turnover.

Apparently, the combination of these two variants leads to a phenotype quite similar to the one reported by Bilguvar *et al.*, which was caused by a homozygous presumed loss-of-function variant. However, despite similarities regarding neurological dysfunction, the cognitive abilities of the patients in the present study were conspicuously well preserved, in contrast to the patients described by Bilguvar *et al.* who had IQ-scores of 71 and 74 (14). The contrast between the cognitive function in the two families is striking, but it is important to bear in mind that this may be due to factors not related to the *UCHL1* mutation. In particular, the high degree of consanguinity in the Turkish family may be a contributing factor to this, with several homozygous segments shared by the affected individuals.

Neuropsychological testing of the twins revealed that in particular the memory function, reflecting mainly hippocampal function, was above norm, while executive functions and language processing, representing frontal and temporal brain areas, were at an average level. The UCHL1 protein level is reduced in the hippocampus in an Alzheimer mouse model and overexpression of UCHL1 has shown to have a rescuing function (7,35). We speculate that the increased activity of the Arg178Gln variant might actually have a protective effect on cognitive function. If so, this supports that overexpression of UCHL1 in the brain could be a promising disease-modifying strategy for Alzheimer's disease (7). On the other hand, UCHL1 dysregulation is also reported in a variety of cancers, although its role is still unclear. Both low expression (36,37) and overexpression have been described. Furthermore, *UCHL1* is a potent oncogene in mice (38). An interesting finding was the two types of cancer in the sister (III-2) heterozygous for the activating Arg178Gln variant. To explore the potential impact of the Arg178Gln variant both in neuroprotection and in cancer pathogenesis, further studies are necessary.

We speculate that the non-soluble Ala216Asp variant results in reduction of functional UCHL1 protein and contributes to neurodegeneration, while the increased enzymatic activity of the Arg178Gln variant might compensate and even protect cognitive function. This, and the diverging results of UCHL1 deregulation in cancer, underlines the complexity of UCHL1 biochemistry.

Conclusions

This study reports the second family with early-onset progressive neurodegeneration with optical atrophy and mutations in *UCHL1*. This finding corroborates that mutations in *UCHL1* are the cause of this rare phenotype, and should be considered in the work-up of patients with early-onset optic atrophy and subsequent progressive neurodegenerative symptoms. Whereas biallelic loss of function seems to cause neurodegenerative disease with reduced cognitive function, we speculate whether the increased hydrolytic activity of the small amount of expressed UCHL1 in our patients might explain their remarkably well preserved memory functions. This observation may encourage future research on increasing UCHL1 activity without altering protein levels in drug and treatment development. This novel mechanistic insight into ubiquitin processing may also apply to other neurodegenerative disorders suffering from protein aggregation, such as Alzheimer's and Parkinson's disease.

Materials and Methods

Clinical investigations

The study was approved by the Regional Ethical Committee for Medical and Health Research Ethics, South-Eastern Norway. Informed consent was obtained from each study participant.

Identifying UCHL1 variants by whole exome sequencing

Over the years extensive investigations were done to identify the molecular diagnosis in this family. A large number of potential diagnoses had previously been excluded, including the most common hereditary spastic paraplegias and hereditary ataxias, relevant mitochondriopathies and metabolic disorders. Whole exome sequencing was performed in siblings III-4 and III-6. We performed targeted enrichment of the exome using the Agilent SureSelect Human All Exon kit v4. Sequencing was performed on an Illumina HiSeq2000 with 100 bp paired-end reads. Reads were aligned to the reference human genome (hg19) using Novoalign (V2.07.17) (http://www.novocraft.com/products/novoalign) and the Genome Analysis Toolkit (GATK, v2.4-9) (39,40). Variant calling was performed using GATK (v2.4-9). Variants were annotated by ANNOVAR (41). Downstream filtering and analysis was done in FILTUS (42), using allele frequencies, conservation scores (GERP) and various *in silico* prediction tools (43–46) to search for pathogenic variants compatible with recessive inheritance. Sanger sequencing of the *UCHL1* variants was performed in all siblings (III-1-6), and in 177 healthy Norwegian blood-donors (primer sequences available on request). An in-house database of 441 exomes was also screened for the variants. In a parallel project, high-throughput sequencing of *UCHL1* exons in 113 probands with spinocerebellar disorders and 230 healthy individuals was performed, as described by Pihlstrøm *et al.* (47).

Cloning of human wild type UCHL1 and mutants

cDNAs encoding full length human wild type (WT) UCHL1 and the two mutants Arg178Gln and Ala216Asp were synthesized with codons optimized for expression in *Escherichia coli* (GenScript). The cDNAs were subcloned into the NcoI-BamHI sites at the Multi Cloning Site of the pETM-11 vector (EMBL collection), which includes an N-terminal His6-tag and a Tobacco Etch Virus (TEV) protease cleavage site in front of the inserted gene.

Expression and purification of UCHL1 constructs

The three different UCHL1 constructs were transformed into *E. coli* BL21 (DE3) RIL Codon Plus cells (Stratagene) for overexpression. Cultures were grown in LB medium. Protein expression was induced when the cell density reached an OD600 of ~0.8 by the addition of isopropyl-β-D-thiogalactopyranoside to a final concentration of 1 mM. Induced cells were grown for 18 h at 18 °C prior to harvesting by centrifugation at 6561*g*. The cell pellets were resuspended in 50 mM Tris pH 7.5 and 300 mM NaCl; the cells were lysed by sonication. Cellular debris was removed by centrifugation at 20217*g*, and the protein was purified by a two-step procedure with Ni-NTA resin preequilibrated with lysis buffer; once before and once after tag cleavage overnight at 4 °C with His-tagged TEV protease. The purified protein was dialyzed against 50 mM Tris pH 7.5 and 100 mM NaCl. Glycerol was added to a final concentration 50% (v/v) and the samples were stored at −20 °C before further use. Of the three constructs, only the WT and the Arg178Gln mutant could be purified. The Ala216Asp mutant protein turned out to be insoluble and accumulated in inclusion bodies (data not shown).

Enzymatic activity assay

WT UCHL1 and the Arg178Gln mutant were diluted into reaction buffer (50 mM Tris-HCl pH 7.5, 1 mM EDTA and 1 mM DTT) in individual wells of a 96-well plate to the final concentration of 4 nM. Ubiquitin-7-amido-4-methycoumarin (ubiquitin-AMC from BostonBiochem) was added to the reaction mixture to yield a final concentration of 2.5 μM to initiate the enzymatic reaction. The rate of AMC cleavage was monitored at 28 °C by a Wallac 1420 VICTOR2™ with excitation at 380 nm and emission at 465 nm.

Preparation of cell lysates

Cell pellets of fibroblasts from a healthy control (BJ (ATCC® CRL-2522™) and patients III-5 and III-6 were lysed as previously described (48) with a few modifications; the lysis buffer did not contain suberoylanilide hydroxamic acid and had 0.01 μM Ubiquitin Aldehyde. After incubation for 1 h at room temperature, remaining cells were disrupted using a MAGNAlyser (Roche) at 5000 rpm for 10 s.

Sample preparation for targeted mass spectrometry

30 μg protein of each cell lysate were incubated with 50 mM NH_4HCO_3 containing 5 mM Tris(2-carboxyethyl)phosphine (TCEP) for 30 min followed by alkylation with 1 μmol/mg protein of iodoacetamide for 30 min in the dark. Proteins were precipitated using a methanol-chloroform method as described (49), resuspended in 30 μl 50 mM NH_4HCO_3 followed by overnight digestion at 37°C with the same volume of trypsin (Thermo Scientific) or Glu-C sequencing grade (Promega) at at 1:50 ratios and 1:25 (w/w,

enzyme:protein), respectively. Subsequently, formic acid was added to all samples (final concentration 0.1%).

Peptide standards for targeted mass spectrometry

Purified UCHL1 recombinant proteins (WT and the mutant Arg178Gln) and an *E. coli* lysate expressing UCHL1 mutant protein Ala216Asp were used to generate peptide standards for targeted mass spectrometry analysis. Common peptides for WT and mutant proteins were used to represent total UCHL1 proteins. Peptides containing Arg178 or carrying the mutation Arg178Gln as well as Ala216 and the corresponding mutation Ala216Asp were analysed separately and not included in total UCHL1 protein quantification. β-actin peptides generated by enzymatic digestion of human fibroblast cells were used as internal standard for data normalization.

Targeted mass spectrometry

Parallel reaction monitoring (PRM)-based targeted mass spectrometry methods were performed as previously described (48) with minor modifications. Peptides were analysed in a Q Exactive mass spectrometer coupled to an Easy-nLC 1000 UHPLC system (Thermo Scientific). Peptides were injected onto an Acclaim PepMap100 C-18 column and further separated on an Acclaim PepMap100 C-18 analytical column (Thermo Scientific). A 120 min method was used at a 250 nl/min flow rate: starting with 98% buffer A (0.1% formic acid) with an increase to 5% buffer B (100% acetonitrile, 0.1% formic acid) in 2 min, followed by an increase to 35% B over 102 min and a rapid increase to 100% B in 6 min, where it was subsequently held for 10 min. Peptides eluting from the column were analysed on the Q Exactive operating in t-MS2 mode (48).

Experimental design, data analysis and processing were performed using the Skyline software version 3.1.0.7382 (50). Briefly, *in silico* selection of proteotypic peptides was performed via Skyline using the Homo sapiens reference proteome available at www.uniprot.org to exclude non-unique peptides. Peptide standards were first analysed in a Q Exactive and the data was imported into Skyline where the top 2–8 ionizing peptides (2+ or 3+ charge states) were selected for PRM analysis. Here, information on retention time and fragmentation pattern of the standards was used to identify the peptides for each protein and to build a scheduled PRM method with a retention time window of 15 min. The method was then used for detection and quantification of corresponding peptides in patient samples and the sum of the integrated peak areas of the most intense fragments was used for peptide quantification. For total UCHL1 protein and β-actin, which was employed as internal standard for data normalization, peptide areas for multiple peptides of the same protein were summed to assign relative abundance to that protein. Levels of mutant peptides and corresponding WT peptides were assigned according to single peptides carrying the corresponding residues. The error bars represent the standard deviation of 3 technical replicates.

Acknowledgements

We thank the family for participating in our studies, Dr. L. Pihlstrøm and Dr. M. Toft for gene panel analyses and results, Dr. M. Chawla for neuroradiological assistance and Ole Boye for assistance with protein expression and purification.

Conflict of Interest Statement. None Declared.

Funding

This work was supported by the Department of Neurology, Oslo University Hospital, South-Eastern Health Region Grants [grant 2011057, KKS and ZI] and Structural Biology Core Facility of South-Eastern Health region. The Proteomics and Metabolomics Core Facility PROMEC is funded by NTNU and the Central Norway Regional Health Authority.

References

1. Jayadev, S. and Bird, T.D. (2013) Hereditary ataxias: overview. *Genet. Med.*, **15**, 673–683.
2. Klebe, S., Stevanin, G. and Depienne, C. (2015) Clinical and genetic heterogeneity in hereditary spastic paraplegias: from SPG1 to SPG72 and still counting. *Rev. Neurol. (Paris)*, **171**, 505–530.
3. Schofield, J.N., Day, I.N., Thompson, R.J. and Edwards, Y.H. (1995) PGP9.5, a ubiquitin C-terminal hydrolase; pattern of mRNA and protein expression during neural development in the mouse. *Brain Res. Dev. Brain Res.*, **85**, 229–238.
4. Wilkinson, K.D., Lee, K.M., Deshpande, S., Duerksen-Hughes, P., Boss, J.M. and Pohl, J. (1989) The neuron-specific protein PGP 9.5 is a ubiquitin carboxyl-terminal hydrolase. *Science*, **246**, 670–673.
5. Jackson, P. and Thompson, R.J. (1981) The demonstration of new human brain-specific proteins by high-resolution two-dimensional polyacrylamide gel electrophoresis. *J. Neurol. Sci.*, **49**, 429–438.
6. Liu, Y., Fallon, L., Lashuel, H.A., Liu, Z. and Lansbury, P.T. Jr. (2002) The UCH-L1 gene encodes two opposing enzymatic activities that affect alpha-synuclein degradation and Parkinson's disease susceptibility. *Cell*, **111**, 209–218.
7. Zhang, M., Cai, F., Zhang, S., Zhang, S. and Song, W. (2014) Overexpression of ubiquitin carboxyl-terminal hydrolase L1 (UCHL1) delays Alzheimer's progression in vivo. *Sci. Rep.*, **4**, 7298.
8. Ragland, M., Hutter, C., Zabetian, C. and Edwards, K. (2009) Association between the ubiquitin carboxyl-terminal esterase L1 gene (UCHL1) S18Y variant and Parkinson's Disease: a HuGE review and meta-analysis. *Am. J. Epidemiol.*, **170**, 1344–1357.
9. Liu, Y., Chen, Y.Y., Liu, H., Yao, C.J., Zhu, X.X., Chen, D.J., Yang, J., Lu, Y.J. and Cao, J.Y. (2015) Association between ubiquitin carboxy-terminal hydrolase-L1 S18Y variant and risk of Parkinson's disease: the impact of ethnicity and onset age. *Neurol. Sci.*, **36**, 179–188.
10. Butterfield, D.A., Gnjec, A., Poon, H.F., Castegna, A., Pierce, W.M., Klein, J.B. and Martins, R.N. (2006) Redox proteomics identification of oxidatively modified brain proteins in inherited Alzheimer's disease: an initial assessment. *J. Alzheimers Dis.*, **10**, 391–397.
11. Jara, J.H., Frank, D.D. and Ozdinler, P.H. (2013) Could dysregulation of UPS be a common underlying mechanism for cancer and neurodegeneration? Lessons from UCHL1. *Cell Biochem. Biophys.*, **67**, 45–53.
12. Leroy, E., Boyer, R., Auburger, G., Leube, B., Ulm, G., Mezey, E., Harta, G., Brownstein, M.J., Jonnalagada, S., Chernova, T., *et al.* (1998) The ubiquitin pathway in Parkinson's disease. *Nature*, **395**, 451–452.
13. Wintermeyer, P., Kruger, R., Kuhn, W., Muller, T., Woitalla, D., Berg, D., Becker, G., Leroy, E., Polymeropoulos, M., Berger, K., *et al.* (2000) Mutation analysis and association studies of

the UCHL1 gene in German Parkinson's disease patients. *Neuroreport*, **11**, 2079–2082.
14. Bilguvar, K., Tyagi, N.K., Ozkara, C., Tuysuz, B., Bakircioglu, M., Choi, M., Delil, S., Caglayan, A.O., Baranoski, J.F., Erturk, O., *et al.* (2013) Recessive loss of function of the neuronal ubiquitin hydrolase UCHL1 leads to early-onset progressive neurodegeneration. *Proc. Natl. Acad. Sci. U. S. A*, **110**, 3489–3494.
15. Chen, F., Sugiura, Y., Myers, K.G., Liu, Y. and Lin, W. (2010) Ubiquitin carboxyl-terminal hydrolase L1 is required for maintaining the structure and function of the neuromuscular junction. *Proc. Natl. Acad. Sci. U. S. A*, **107**, 1636–1641.
16. Nyberg-Hansen, R. and Refsum, S. (1972) Spastic paraparesis associated with optic atrophy in monozygotic twins. *Acta Neurol. Scand. Suppl.*, **51**, 261–263.
17. Schule, R., Holland-Letz, T., Klimpe, S., Kassubek, J., Klopstock, T., Mall, V., Otto, S., Winner, B. and Schols, L. (2006) The Spastic Paraplegia Rating Scale (SPRS): a reliable and valid measure of disease severity. *Neurology*, **67**, 430–434.
18. Schmitz-Hubsch, T., du Montcel, S.T., Baliko, L., Berciano, J., Boesch, S., Depondt, C., Giunti, P., Globas, C., Infante, J., Kang, J.S., *et al.* (2006) Scale for the assessment and rating of ataxia: development of a new clinical scale. *Neurology*, **66**, 1717–1720.
19. Das, C., Hoang, Q.Q., Kreinbring, C.A., Luchansky, S.J., Meray, R.K., Ray, S.S., Lansbury, P.T., Ringe, D. and Petsko, G.A. (2006) Structural basis for conformational plasticity of the Parkinson's disease-associated ubiquitin hydrolase UCH-L1. *Proc. Natl. Acad. Sci. U. S. A*, **103**, 4675–4680.
20. Bourmaud, A., Gallien, S. and Domon, B. (2016) Parallel reaction monitoring using quadrupole-Orbitrap mass spectrometer: Principle and applications. *Proteomics*, **16**, 2146–2159.
21. Gallien, S. and Domon, B. (2015) Advances in high-resolution quantitative proteomics: implications for clinical applications. *Expert Rev. Proteomics*, **12**, 489–498.
22. Peterson, A.C., Russell, J.D., Bailey, D.J., Westphall, M.S. and Coon, J.J. (2012) Parallel reaction monitoring for high resolution and high mass accuracy quantitative, targeted proteomics. *Mol. Cell. Proteomics*, **11**, 1475–1488.
23. Genç, B., Jara, J.H., Schultz, M.C., Manuel, M., Stanford, M.J., Gautam, M., Klessner, J.L., Sekerkova, G., Heller, D.B., Cox, G.A., *et al.* (2016) Absence of UCHL 1 function leads to selective motor neuropathy. *Ann. Clin. Trans. Neurol.*, **3**, 331–345.
24. Yasuda, T., Nihira, T., Ren, Y.R., Cao, X.Q., Wada, K., Setsuie, R., Kabuta, T., Wada, K., Hattori, N., Mizuno, Y., *et al.* (2009) Effects of UCH-L1 on alpha-synuclein over-expression mouse model of Parkinson's disease. *J. Neurochem.*, **108**, 932–944.
25. Delettre, C., Lenaers, G., Griffoin, J.M., Gigarel, N., Lorenzo, C., Belenguer, P., Pelloquin, L., Grosgeorge, J., Turc-Carel, C., Perret, E., *et al.* (2000) Nuclear gene OPA1, encoding a mitochondrial dynamin-related protein, is mutated in dominant optic atrophy. *Nat. Genet.*, **26**, 207–210.
26. Larsson, N.G., Andersen, O., Holme, E., Oldfors, A. and Wahlstrom, J. (1991) Leber's hereditary optic neuropathy and complex I deficiency in muscle. *Ann. Neurol.*, **30**, 701–708.
27. Casari, G., De Fusco, M., Ciarmatori, S., Zeviani, M., Mora, M., Fernandez, P., De Michele, G., Filla, A., Cocozza, S., Marconi, R., *et al.* (1998) Spastic paraplegia and OXPHOS impairment caused by mutations in paraplegin, a nuclear-encoded mitochondrial metalloprotease. *Cell*, **93**, 973–983.
28. Wedding, I.M., Koht, J., Tran, G.T., Misceo, D., Selmer, K.K., Holmgren, A., Frengen, E., Bindoff, L., Tallaksen, C.M. and Tzoulis, C. (2014) Spastic paraplegia type 7 is associated with multiple mitochondrial DNA deletions. *PLoS One*, **9**, e86340.
29. Klebe, S., Depienne, C., Gerber, S., Challe, G., Anheim, M., Charles, P., Fedirko, E., Lejeune, E., Cottineau, J., Brusco, A., *et al.* (2012) Spastic paraplegia gene 7 in patients with spasticity and/or optic neuropathy. *Brain*, **135**, 2980–2993.
30. Sanchez-Ferrero, E., Coto, E., Beetz, C., Gamez, J., Corao, A.I., Diaz, M., Esteban, J., del Castillo, E., Moris, G., Infante, J., *et al.* (2013) SPG7 mutational screening in spastic paraplegia patients supports a dominant effect for some mutations and a pathogenic role for p.A510V. *Clin. Genet.*, **83**, 257–262.
31. Rydning, S.L., Wedding, I.M., Koht, J., Chawla, M., Oye, A.M., Sheng, Y., Vigeland, M.D., Selmer, K.K. and Tallaksen, C.M. (2016) A founder mutation p.H701P identified as a major cause of SPG7 in Norway. *Eur. J. Neurol.*, **23**, 763–771.
32. Bennett, E.J., Shaler, T.A., Woodman, B., Ryu, K.Y., Zaitseva, T.S., Becker, C.H., Bates, G.P., Schulman, H. and Kopito, R.R. (2007) Global changes to the ubiquitin system in Huntington's disease. *Nature*, **448**, 704–708.
33. Tramutola, A., Di Domenico, F., Barone, E., Perluigi, M. and Butterfield, D.A. (2016) It Is All about (U)biquitin: Role of Altered Ubiquitin-Proteasome System and UCHL1 in Alzheimer Disease. *Oxid. Med. Cell. Longev*, **2016**, 2756068.
34. McNaught, K.S. and Jenner, P. (2001) Proteasomal function is impaired in substantia nigra in Parkinson's disease. *Neurosci. Lett.*, **297**, 191–194.
35. Gong, B., Cao, Z., Zheng, P., Vitolo, O.V., Liu, S., Staniszewski, A., Moolman, D., Zhang, H., Shelanski, M. and Arancio, O. (2006) Ubiquitin hydrolase Uch-L1 rescues beta-amyloid-induced decreases in synaptic function and contextual memory. *Cell*, **126**, 775–788.
36. Bonazzi, V.F., Nancarrow, D.J., Stark, M.S., Moser, R.J., Boyle, G.M., Aoude, L.G., Schmidt, C. and Hayward, N.K. (2011) Cross-platform array screening identifies COL1A2, THBS1, TNFRSF10D and UCHL1 as genes frequently silenced by methylation in melanoma. *PLoS One*, **6**, e26121.
37. Jin, C., Yu, W., Lou, X., Zhou, F., Han, X., Zhao, N. and Lin, B. (2013) UCHL1 Is a Putative Tumor Suppressor in Ovarian Cancer Cells and Contributes to Cisplatin Resistance. *J. Cancer*, **4**, 662–670.
38. Hussain, S., Bedekovics, T., Chesi, M., Bergsagel, P.L. and Galardy, P.J. (2015) UCHL1 is a biomarker of aggressive multiple myeloma required for disease progression. *Oncotarget.*, **6**, 40704–40718.
39. DePristo, M.A., Banks, E., Poplin, R., Garimella, K.V., Maguire, J.R., Hartl, C., Philippakis, A.A., del Angel, G., Rivas, M.A., Hanna, M., *et al.* (2011) A framework for variation discovery and genotyping using next-generation DNA sequencing data. *Nat. Genet.*, **43**, 491–498.
40. McKenna, A., Hanna, M., Banks, E., Sivachenko, A., Cibulskis, K., Kernytsky, A., Garimella, K., Altshuler, D., Gabriel, S., Daly, M., *et al.* (2010) The Genome Analysis Toolkit: a MapReduce framework for analyzing next-generation DNA sequencing data. *Genome Res.*, **20**, 1297–1303.
41. Wang, K., Li, M. and Hakonarson, H. (2010) ANNOVAR: functional annotation of genetic variants from high-throughput sequencing data. *Nucleic Acids Res.*, **38**, e164.
42. Vigeland, M.D., Gjotterud, K.S. and Selmer, K.K. (2016) FILTUS: a desktop GUI for fast and efficient detection of disease-causing variants, including a novel autozygosity detector. *Bioinformatics*, **32**, 1592–1594.
43. Ng, P.C. and Henikoff, S. (2003) SIFT: Predicting amino acid changes that affect protein function. *Nucleic Acids Res.*, **31**, 3812–3814.
44. Sunyaev, S., Ramensky, V., Koch, I., Lathe, W., 3rd, Kondrashov, A.S. and Bork, P. (2001) Prediction of deleterious human alleles. *Hum. Mol. Genet.*, **10**, 591–597.

45. Ramensky, V., Bork, P. and Sunyaev, S. (2002) Human non-synonymous SNPs: server and survey. *Nucleic Acids Res.*, **30**, 3894–3900.
46. Schwarz, J.M., Cooper, D.N., Schuelke, M. and Seelow, D. (2014) MutationTaster2: mutation prediction for the deep-sequencing age. *Nat. Methods*, **11**, 361–362.
47. Pihlstrom, L., Rengmark, A., Bjornara, K.A. and Toft, M. (2014) Effective variant detection by targeted deep sequencing of DNA pools: an example from Parkinson's disease. *Ann. Hum. Genet.*, **78**, 243–252.
48. Pettersen, H.S., Galashevskaya, A., Doseth, B., Sousa, M.M., Sarno, A., Visnes, T., Aas, P.A., Liabakk, N.B., Slupphaug, G., Saetrom, P., *et al.* (2015) AID expression in B-cell lymphomas causes accumulation of genomic uracil and a distinct AID mutational signature. *DNA Repair*, **25**, 60–71.
49. Wessel, D. and Flugge, U.I. (1984) A method for the quantitative recovery of protein in dilute solution in the presence of detergents and lipids. *Anal. Biochem.*, **138**, 141–143.
50. MacLean, B., Tomazela, D.M., Shulman, N., Chambers, M., Finney, G.L., Frewen, B., Kern, R., Tabb, D.L., Liebler, D.C. and MacCoss, M.J. (2010) Skyline: an open source document editor for creating and analyzing targeted proteomics experiments. *Bioinformatics*, **26**, 966–968.